NASA Technical Memorandum 87001

(A-TM-87001) AERODYNAMIC DETUNING N85-26670
A YSIS OF AN UNSTALLED SUPERSONIC TURBOFAN
C DE (NASA) 25 p HC A02/MF A01 CSCL 01A
Unclas
G3/02 21260

Aerodynamic Detuning Analysis of an Unstalled Supersonic Turbofan Cascade

Daniel Hoyniak
Lewis Research Center
Cleveland, Ohio

and

Sanford Fleeter
Purdue University
West Lafayette, Indiana

Prepared for the
Thirtieth International Gas Turbine Conference and Exhibit
sponsored by the American Society of Mechanical Engineers
Houston, Texas, March 17-21, 1985

NASA

AERODYNAMIC DETUNING ANALYSIS OF AN UNSTALLED SUPERSONIC TURBOFAN CASCADE

Daniel Hoyniak
National Aeronautics and Space Administration
Lewis Research Center
Cleveland, Ohio 44135

and

Sanford Fleeter
School of Mechanical Engineering
Purdue University
West Lafayette, Indiana

E-2546

SUMMARY

A new, and as yet unexplored, approach to passive flutter control is aerodynamic detuning, defined as designed passage-to-passage differences in the unsteady aerodynamic flow field of a rotor blade row. Thus, aerodynamic detuning directly affects the fundamental driving mechanism for flutter, i.e., the unsteady aerodynamic forces and moments acting on individual rotor blades. In this paper, a model to demonstrate the enhanced supersonic unstalled aeroelastic stability associated with aerodynamic detuning is developed. The stability of an aerodynamically detuned cascade operating in a supersonic inlet flow field with a subsonic leading edge locus is analyzed, with the aerodynamic detuning accomplished by means of nonuniform circumferential spacing of adjacent rotor blades. The unsteady aerodynamic forces and moments on the blading are defined in terms of influence coefficients in a manner that permits the stability of both a conventional uniformally spaced rotor configuration as well as the detuned nonuniform circumferentially spaced rotor to be determined. With Verdon's uniformly spaced Cascade B as a baseline, this analysis is then utilized to demonstrate the potential enhanced aeroelastic stability associated with this particular type of aerodynamic detuning.

NOMENCLATURE

c	airfoil chord
i	$\sqrt{-1}$
k	reduced frequency, $k = \omega c/u_\infty$
u_∞	cascade inlet velocity
y_s	mean airfoil position
C	perturbation sonic velocity
$C_{\alpha\alpha}$	unsteady aerodynamic moment coefficient
C_M^n	influence coefficient of airfoil, n

C_p $\frac{p}{1/2\rho u_\infty^2}$

ΔC_p $\frac{\Delta p}{1/2\rho u_\infty^2}$

M dimensionless unsteady aerodynamic moment

M_∞ cascade inlet Mach number

P perturbation pressure

ΔP perturbation pressure difference

S uniform airfoil spacing

S_d nonuniform airfoil spacing

U perturbation chordwise velocity

V perturbation normal velocity

α amplitude of oscillation

$\hat{\alpha}$ complex oscillatory amplitude

β interblade phase angle

ε level of aerodynamic detuning

ζ cascade stagger angle

ρ fluid density

ω oscillatory frequency

[] matrix

Subscripts:

d detuned cascade

n airfoil number

R reference airfoil uniformly spaced cascade

R_e reference for set of even numbered airfoils of detuned cascade

R_o reference for set of odd numbered airfoils of detuned cascade

INTRODUCTION

Structural detuning is defined as blade-to-blade differences in the natural frequencies of a blade row resulting from variations in the individual blade structural properties. Mathematical models have been developed which demonstrate that even the small amounts of blade-to-blade structural detuning associated with manufacturing tolerances can have a beneficial effect on the flutter characteristics of rotor assemblies (refs. 1 to 5). Furthermore, these models indicate that the aeroelastic stability of a rotor can be controlled by the deliberate introduction of increased levels of blade-to-blade structural detuning in the rotor design.

However, blade-to-blade structural detuning is not a universally accepted potential mechanism to eliminate flutter from the operating range of a fan or compressor stage. This is because of the associated manufacturing, material, inventory, engine maintenance, control, and cost problems.

A new, and as yet unexplored, approach to passive, flutter control is aerodynamic detuning, defined as designed passage-to-passage differences in the unsteady aerodynamic flow field of a rotor blade row. Thus, aerodynamic detuning results in blade-to-blade differences in the unsteady aerodynamic forces and moments acting on a blade row. This results in the blading not responding in a classical traveling wave mode typical of the flutter behavior of a conventional aerodynamically tuned rotor. Thus, aerodynamic detuning directly affects the fundamental driving mechanism for flutter, the unsteady aerodynamic forces and moments acting on individual rotor blades.

Supersonic unstalled flutter is a significant, problem in the development of advanced gas turbine fans and compressors because it restricts the high-speed operating range of the engine. Hence, the objective of this research program is to develop a model for aerodynamic detuning applicable to supersonic unstalled flutter. In particular, a mathematical model is developed to analyze the stability of an aerodynamically detuned rotor operating in a supersonic inlet flow field with a subsonic leading edge locus, with the aerodynamic detuning accomplished by means of nonuniform circumferential spacing of adjacent rotor blades. This method of aerodynamic detuning was selected because small solidity variations do not have a dominant effect on the steady-state aerodynamic performance of a rotor. In this model, the unsteady aerodynamic forces and moments acting on the blading are defined in terms of influence coefficients in a manner that permits the stabilty of both a conventional aerodynamically tuned rotor configuration as well as the detuned nonuniform circumferentially spaced rotor to be determined.

UNSTEADY AERODYNAMIC MODEL

Current aeroelastic stability analyses of conventional aerodynamically tuned and structurally detuned rotors utilize two-dimensional aerodynamic models applied in a strip theory technique. Hence, a two-dimensional, uniformly spaced, airfoil cascade is used to represent a typical rotor blade section. These models then analyze the unsteady aerodynamics associated with the airfoil cascade executing harmonic oscillations in a classical traveling wave mode, i.e., with a constant interblade phase angle β between adjacent airfoils.

For supersonic unstalled flutter, a flat plate airfoil cascade embedded in a supersonic inlet flow field with a subsonic leading edge locus (fig. 1) undergoing torsion mode harmonic oscillation is considered. The fluid is assumed to be an inviscid, perfect gas with the flow isentropic, adiabatic, and irrotational. The unsteady continuity and Euler equations are linearized by assuming that the unsteady perturbations are small as compared to the uniform throughflow. Thus, the boundary conditions, which require the unsteady flow to be tangent to the blade and the normal velocity to be continuous across the wake, are applied on the mean positions of the oscillating airfoils.

Unsteady cascade aerodynamics and, in particular, the unsteady forces and moments acting on the uniformly spaced airfoils are then predicted using various techniques, for example (refs. 6 to 14). Of particular interest are the analyses of Verdon (ref. 6), Brix and Platzer (ref. 9), and Caruthers (ref. 10). These analyses utilize a finite cascade representation of the semi-infinite cascade. The cascade periodicity condition is enforced by stacking sufficient numbers of uniformly spaced single airfoils until convergence in the unsteady flow field is achieved.

For the aerodynamically detuned, alternate nonuniform circumferentially spaced rotor, an analogous unsteady aerodynamic model is utilized. In particular, the unsteady aerodynamics associated with the small perturbation torsion mode harmonic oscillations of a nonuniformly spaced two-dimensional flat plate airfoil cascade embedded in an inviscid, supersonic inlet flow field with a subsonic leading edge locus is considered.

The analysis of this type of configuration is most easily accomplished utilizing a finite cascade representation of the semi-infinite cascade (fig. 2). As seen, there are two distinct flow passages: a reduced spacing or increased solidity passage and an increased spacing or reduced solidity passage. Also, the detuned cascade is composed of two separate sets of airfoils. For convenience, these are termed the set of even numbered airfoils and the set of odd numbered airfoils. Thus, two passage periodicity is required for this detuned cascade, i.e., the periodic cascade unsteady flow field is achieved by stacking sufficient numbers of two nonuniform flow passages or two airfoils, one from each set.

For the alternate nonuniform airfoil spacing aerodynamic detuning technique being considered, the spacing, S_d, of the two sets of airfoils is equal (fig. 2). Thus, the individual sets of odd and even numbered airfoils can be considered as cascades of uniformly spaced airfoils each with twice the spacing of the associated baseline uniformly spaced cascade. This enables an interblade phase angle for this aerodynamically detuned cascade configuration to be defined. In particular, each set of airfoils is assumed to be executing harmonic torsional oscillations with a constant interblade phase angle, β_d, between adjacent airfoils. Thus, this detuned cascade interblade phase angle is twice that for the corresponding baseline uniformly spaced cascade. The interblade phase angle for the motion between the sets of even numbered and odd numbered airfoils is determined from the flutter mode which is obtained by specifying the detuned cascade phase angle, β_d, and the level of aerodynamic detuning, ϵ, which defines the nonuniform airfoil spacing.

$$S_{1,2} = (1 \mp \epsilon)S \tag{1}$$

where S is the spacing of the baseline uniformly spaced cascade and S_1 and S_2 denote the spacing of the reduced and increased flow passages of the detuned cascade.

The formulation of the linearized differential equations describing the unsteady perturbation quantities for the finite aerodynamically detuned cascade is based on the method of characteristics analysis of the finite uniformly spaced airfoil cascade developed by Brix and Platzer (ref. 9). In particular the dependent variables are the nondimensional chordwise, normal, and sonic perturbation velocities, U, V, and C, respectively. The independent variables are the dimensionless chordwise and normal coordinates, x and y as defined in figures 1 and 2 and time t. Assuming harmonic motion at a frequency ω, the resulting set of differential equations which describe the unsteady perturbation flow field are specified in equation (2).

$$\frac{\partial U}{\partial x} + \sqrt{M_\infty^2 - 1}\,\frac{\partial V}{\partial y} + \frac{\partial C}{\partial x} + ikM_\infty^2 C = 0 \tag{2a}$$

$$\frac{\partial U}{\partial x} + \frac{\partial C}{\partial y} + ikU = 0 \tag{2b}$$

$$\frac{\partial U}{\partial y} - \sqrt{M_\infty^2 - 1}\,\frac{\partial V}{\partial x} = 0 \tag{2c}$$

Solutions to this system of equations are obtained by the method of characteristics. The compatibility equations are specified in equation 3.

$$\left[\frac{dU}{dx}\right]_\zeta - \left[\frac{dV}{dx}\right]_\zeta + \frac{ikM_\infty^2}{M_\infty^2 - 1}(U - C) = 0 \tag{3a}$$

$$\left[\frac{dU}{dx}\right]_\eta - \left[\frac{dV}{dx}\right]_\eta + \frac{ikM_\infty^2}{M_\infty^2 - 1}(U - C) = 0 \tag{3b}$$

$$\left[\frac{dU}{dx}\right]_{str} + \left[\frac{dC}{dx}\right]_{str} + ikU = 0 \tag{3c}$$

where the subscripts ζ, η, and str indicate that the relation is valid along the left or right running characteristic and the characteristic in the streamline direction, respectively.

The flow tangency boundary condition requires that the normal perturbation velocity component, V, be equal to the normal velocity of the airfoil surfaces on the mean position of the oscillating airfoils. For an aerodynamically detuned airfoil cascade executing harmonic torsional motions about an elastic axis located at x_0 as measured from the leading edge, the dimensionless normal perturbation velocity component on the n-th airfoil is specified in equation (4).

$$V_n(x, y_s, t) = -\alpha_n \left\{1 + (x - x_0)ik\right\} e^{i(kt+n\beta_d)} \tag{4}$$

where y_s denotes the mean position of the airfoils, k is the reduced frequency, β is the interblade phase angle, and α_n denotes the amplitude of oscillation of the n-th airfoil.

These boundary conditions are applied on the mean positions of the oscillating cascaded airfoils. For the uniformly spaced cascade depicted in figure 1, the mean position of the n-th airfoil is given in equation (5).

$$nd \tan \zeta < x < nd \tan \zeta + 1 \qquad (5a)$$

$$y_s = nd \qquad (5b)$$

$$n = 0, \pm 1, \pm 2, \ldots$$

where d is the perpendicular distance between adjacent airfoils, as indicated in figure 1.

For the nonuniformly spaced airfoil cascade depicted in figure 2, the mean position of the n-th even numbered airfoil is specified in equation 6.

$$d_1 + d_2 = D \qquad (6a)$$

$$\left[\frac{n}{2}\right] D \tan \zeta < x < \left[\frac{n}{2}\right] D \tan \zeta + 1 \qquad (6b)$$

$$y_s = \left[\frac{n}{2}\right] D \qquad (6c)$$

The mean positions of the set of odd numbered airfoils can be expressed in an analogous manner.

Thus, the formulation of the mathematical problem for the unsteady aerodynamic model of the alternate nonuniform circumferentially spaced detuned cascade is complete. At the intersection points of the characteristics, equation (3) represents a system of three differential equations in three unknowns, with the appropriate boundary conditions specified in equations (4) and (6). The unknown chordwise, normal, and sonic dimensionless perturbation velocities, U, V, and C, in each of the two periodic flow passages of the semi-infinite cascade are then determined by means of the two airfoil passage stacking technique in conjunction with the finite difference scheme developed by Brix and Platzer for the tuned cascade configuration.

The dimensionless unsteady perturbation pressure distributions on the surfaces of a reference airfoil from each set in the periodic detuned cascade are defined by these perturbation velocities. In particular, these perturbation unsteady surface pressure distributions are determined by means of the linearized unsteady Bernoulli equation. The nondimensional unsteady aerodynamic moment acting on the reference airfoil, M_R, and the standard torsion mode unsteady aerodynamic moment coefficient, $C_{\alpha\alpha}$, are then calculated by integrating the unsteady surface perturbation pressure difference across the chordline per equation (7).

$$M_R = \int_0^1 \Delta P(x,\ y_s,\ t)(x - x_0)dx = C_{\alpha\alpha}\alpha_R e^{i\omega t} \tag{7}$$

where α_R is the amplitude of oscillation of the reference airfoil.

INFLUENCE COEFFICIENT TECHNIQUE

The boundary conditions specified in equations (4) and (6) require that the nonuniformly spaced airfoils oscillate with equal amplitudes, a situation not appropriate for the detuned airfoil cascade. In addition, the application of this analysis is unnecessarily costly because the complete periodic perturbation flow field must be recalculated, not only for every new cascade geometry and flow condition, but also for each interblade phase angle value considered for a particular cascade and flow condition. These limitations are easily rectified by calculating the unsteady aerodynamic moment coefficients, $C_{\alpha\alpha}$, by means of influence coefficients. This influence coefficient technique will first be developed for a cascade of uniformly spaced airfoils and then extended for the aerodynamically detuned nonuniformly spaced cascade.

For an aerodynamically tuned cascade with N uniformly spaced airfoils, the total unsteady aerodynamic moment acting on an arbitrary reference airfoil, M_R, can be expressed in terms of influence coefficients per equation (8).

$$M_R = \hat{\alpha}_0 \left[C_M^0\right]_R + \hat{\alpha}_1 \left[C_M^1\right]_R + \ldots + \hat{\alpha}_R \left[C_M^R\right]_R + \ldots + \hat{\alpha}_N \left[C_M^N\right]_R \tag{8}$$

Here, $\left[C_M^n\right]_R$ denotes the influence coefficients on the reference airfoil, R, associated with the motion of airfoil number n. Physically it represents the unsteady aerodynamic moment acting on the fixed reference airfoil, R, due to a unit amplitude torsional oscillation of airfoil number n. When n corresponds to R, the influence coefficient $\left[C_M^R\right]_R$ is the unsteady moment acting on airfoil R due to its own motion, with all other airfoils fixed.

For the detuned nonuniformly spaced cascade, a reference flow passage bounded by two reference airfoils must be considered. This is because the detuned cascade is made up of two distinct sets of airfoils, termed the odd numbered and the even numbered airfoils, and two distinct flow passages. Each of these flow passages is bounded by one airfoil from each airfoil set, per figure 3.

A reduced spacing flow passage is taken as the reference. The reference airfoil for the lower boundary of the reference flow passage and for the set of even numbered airfoils is denoted by R_e. The reference airfoil for the upper boundary of the reference flow passage and for the set of odd numbered airfoils is denoted by R_o. Thus, the unsteady aerodynamic moment acting on these two reference airfoils can each be written in terms of the influence of the sets of odd and even numbered airfoils as follows.

$$M_{R_o,R_e} = \hat{\alpha}_1 \left[C_M^1\right]_{R_o,R_e} + \hat{\alpha}_3 \left[C_M^3\right]_{R_o,R_e} + \ldots$$

$$+ \hat{\alpha}_{R_o} \left[C_M^{R_o}\right]_{R_o,R_e} + \ldots + \hat{\alpha}_N \left[C_M^N\right]_{R_o,R_e}$$

$$+ \hat{\alpha}_0 \left[C_M^0\right]_{R_o,R_e} + \hat{\alpha}_2 \left[C_M^2\right]_{R_o,R_e} + \ldots$$

$$+ \hat{\alpha}_{Re} \left[C_M^{Re}\right]_{R_o,R_e} + \ldots + \hat{\alpha}_{N-1} \left[C_M^{N-1}\right]_{R_o,R_e} \quad (9)$$

The two groups of bracketed terms are associated with the motion of the sets of odd numbered and even numbered airfoils, respectively. Also, to assure that there are an equal number of reduced spacing and increased spacing flow passages in the cascade, i.e., that periodicity is achieved by stacking two airfoil passages at a time, equation (9) has been developed assuming that the cascade is made up of an odd number of airfoils, thereby resulting in an even number of airfoil passages.

The amplitude of the harmonic oscillations of the set of odd numbered airfoils is denoted by $\hat{\alpha}_{R_o}$ exp(in β_d), with β_d defining the constant interblade phase angle between sequentially odd numbered airfoils. The set of even numbered airfoils are assumed to oscillate with a complex amplitude $\hat{\alpha}_{R_e}$ exp(in β_d), with the same constant interblade phase angle. The amplitude and phase difference between the motions of the sets of odd and even numbered airfoils is accounted for by considering the amplitudes of oscillation, $\hat{\alpha}_{R_o}$ and $\hat{\alpha}_{R_e}$, to be complex quantities. Because the interblade phase angles are referenced to the reference airfoils, R_o and R_e, the dimensionless unsteady aerodynamic momnets, equation (10), are rewritten in terms of the amplitudes of oscillation of the two reference airfoils as follows.

$$M_{R_o,R_e} = \hat{\alpha}_{R_o} \left\{ \left[C_M^{R_o}\right]_{R_o,R_e} + e^{i\beta_d} \left[C_M^3\right]_{R_o,R_e} + \ldots + e^{i\left[\frac{N-1}{2}\right]\beta_d} \left[C_M^N\right]_{R_o,R_e} \right\}$$

$$+ \hat{\alpha}_{R_e} \left\{ \left[C_M^{R_e}\right]_{R_o,R_e} + e^{i\beta_d} \left[C_M^2\right]_{R_o,R_e} + \ldots + e^{i\left[\frac{N-3}{2}\right]\beta_d} \left[C_M^{N-1}\right]_{R_o,R_e} \right\} \quad (10)$$

where the subscripts R_o, R_e refer to the individual reference airfoils.

These two reference airfoil unsteady aerodynamic moments can be shown to be a standard eigenvalue problem, expressed in matrix form as follows.

$$\begin{bmatrix} M_{R_o} \\ \\ M_{R_e} \end{bmatrix} = C_{\alpha\alpha} \begin{bmatrix} \hat{\alpha}_{R_o} \\ \\ \hat{\alpha}_{R_e} \end{bmatrix} = \begin{bmatrix} \left[CM^1\right]_{R_o} & \left[CM^2\right]_{R_o} \\ \\ \left[CM^1\right]_{R_e} & \left[CM^2\right]_{R_e} \end{bmatrix} \begin{bmatrix} \hat{\alpha}_{R_o} \\ \\ \hat{\alpha}_{R_e} \end{bmatrix} \tag{11}$$

where:

$$\left[CM^1\right]_{R_o,R_e} = \left[C_M^{R_o}\right]_{R_o,R_e} + e^{i\beta_d}\left[C_M^3\right]_{R_o,R_e} + \ldots + e^{i\left[\frac{N-1}{2}\right]\beta_d}\left[C_M^N\right]_{R_o,R_e}$$

$$\left[CM^2\right]_{R_o,R_e} = \left[C_M^{R_e}\right]_{R_o,R_e} + e^{i\beta_d}\left[C_M^4\right]_{R_o,R_e} + \ldots + e^{i\left[\frac{N-3}{2}\right]\beta_d}\left[C_M^{N-1}\right]_{R_o,R_e}$$

The terms $\left[CM^1\right]_{R_o,R_e}$ describe the influence that the set of odd numbered airfoils has on the unsteady moment developed on reference airfoils R_o and R_e respectively. $\left[CM^2\right]_{R_o,R_e}$ represents the effect that the set of even numbered airfoils has on these two reference airfoils.

Equation 11 denotes a standard eigenvalue problem. The unsteady aerodynamic moment coefficient, $C_{\alpha\alpha}$, is the eigenvalue of the influence coefficient matrix, [CM], with the associated eigenvector defining the flutter mode for the nonuniformly spaced cascade, i.e., the relationship between the motions of the sets of odd numbered and even numbered airfoils. In the limit wherein this aerodynamically detuned cascade becomes uniformly spaced, the eigenvalue problem of equation (11) reduces exactly to that considered by Bendiksen (ref. 4) for a tuned airfoil cascade.

The influence coefficients $\left[C_M^n\right]_{R_o,R_e}$ are determined from a modification of the unsteady aerodynamic model previously described. For example, to determine $\left[C_M^n\right]_{R_o}$, airfoil n is harmonically oscillated while all of the other nonuniformly spaced cascaded airfoils are kept fixed and the effect on reference airfoil R_o calculated. With all of the influence coefficients determined in this manner, $\left[CM^1\right]_{R_o,R_e}$ and $\left[CM^2\right]_{R_o,R_e}$ are calculated by vector addition of the appropriate influence coefficients after multiplication by the specified complex interblade phase angle term. To analyze a different interblade phase angle, it is only necessary to perform the vector addition in terms of this new phase angle. The influence coefficients calculated from the unsteady aerodynamic model do not have to be recalculated.

Thus, this matrix formulation of the eigenvalue problem (eq. (11)) is utilized herein in conjunction with the influence coefficient technique to efficiently determined the standard dimensionless torsion mode unsteady aerodynamic moment coefficients, $C_{\alpha\alpha}$, for specified aerodynamically tuned and detuned nonuniformly spaced cascade configurations.

MODEL VERIFICATION

To verify the formulation of this aerodynamically detuned finite cascade model, the limiting case of a uniformly spaced cascade configuration is considered. In particular, both this detuned finite cascade analysis based on an influence coefficient technique and the uniformly spaced infinite cascade analysis of Adamczyk and Goldstein (ref. 11) are applied to Verdon's uniformly spaced Cascade B configuration (ref. 14).

The real and imaginary parts of the unsteady aerodynamic moment coefficient, $C_{\alpha\alpha}$, predicted with these two models are presented in figure 4, with the interblade phase angle β as a parameter. Two interblade phase angles are associated with each point shown in figure 4. β_d refers to the interblade phase angle utilized in equation (10) and β is the interblade phase angle calculated from the eigenvectors of equation (11). Because the cascaded airfoils are executing single degree of freedom torsion mode oscillations, the stability of the cascade is specified by the sign of the imaginary part of this moment coefficient, with positive values corresponding to an unstable configuration. As seen, there is excellent agreement between these two analyses for all interblade phase angles.

RESULTS

To demonstrate this nonuniform airfoil spacing technique for aerodynamic detuning, the Cascade B geometry is utilized as a baseline with a midchord elastic axis location.

The influence coefficients, $\left[C_M^n\right]$, for both the uniformly spaced baseline cascade and a 13.3 percent nonuniformly spaced cascade are presented in figure 5. As seen, the airfoils from 0 to $-\infty$ have no influence because of the law of forbidden signals. For the detuned cascade, the reference airfoils R_0 and R_e are oscillated. For comparison purposes, the results are shifted so that the results presented in this figure correspond to airfoil number two being the oscillating reference airfoil in all cases. These influence coefficients are displayed in a manner corresponding to airfoil number 2 harmonically oscillating with all other airfoils in the cascade fixed. As seen, the oscillating airfoil has a significant effect only on the unsteady moments developed on the airfoils in its immediate vicinity. Also, the influence of the oscillating airfoil itself on the total unsteady moment coefficient, $C_{\alpha\alpha}$, is stabilizing. The stabilizing or destabilizing influence of the other airfoils in the cascade can not be determined from these influence coefficients alone. This is because the total unsteady moment coefficient is determined from these influence coefficients by performing the vector addition indicated in equation (11) for a specified interblade phase angle value referenced to the oscillating airfoil.

The variation of $C_{\alpha\alpha}$ with interblade phase angle for both the 13.3 percent nonuniformly spaced detuned cascade and the baseline is presented in figure 6. For the conditions considered, the baseline cascade exhibits an instability, i.e., the imaginary part of $C_{\alpha\alpha}$ has a positive value. However, the aerodynamic detuning associated with this nonuniform spacing results in a neutrally stable or stable configuration for all interblade phase angle values. Also, the nonuniform airfoil spacing generally exhibits a beneficial effect on stability in that this aerodynamic detuning results in the imaginary part of the moment coefficients for the detuned cascade becoming more negative than the corresponding baseline values. This beneficial effect is particularly evident for interblade phase angle values corresponding to forward traveling waves, being somewhat less pronounced for backward traveling waves.

Figure 7 shows the effect of inlet Mach number on the variation with reduced frequency of the imaginary part of $C_{\alpha\alpha}$ for the least stable interblade phase angle value. For a constant Mach number value, the stability of the uniformly spaced baseline configuration is generally enhanced by the nonuniform airfoil spacing, with the larger effects associated with the lower Mach numbers. Also, as the Mach number increases, there is a decreased effect of aerodynamic detuning on the critical reduced frequency, defined as the reduced frequency resulting in neutral stability and characterized by a value of zero for the imaginary part of $C_{\alpha\alpha}$.

To demonstrate the fundamental mechanism for the enhanced stability of the detuned cascade, the reduced frequency and Mach number at which the detuned configuration is neutrally stable but the baseline cascade is unstable is considered: $k = 1.2375$ and $M = 1.15$, per figure 7. The chordwise variation of the imaginary part of the dimensionless surface pressure and pressure differences on the reference airfoils for the detuned and baseline configurations are presented in figures 8 to 13. As seen, the aerodynamic detuning affects the imaginary part of the unsteady surface pressure distributions over the complete airfoil chord, including the surface intersection locations, of the Mach waves and their reflections (figs. 8 to 11). However, there is only a relatively small effect on the chordwise distributions of the unsteady pressure differences in front of the first Mach wave - airfoil intersection location as a result of this aerodynamic detuning (figs. 12 and 13). The effect of aerodynamic detuning on these unsteady pressure difference distributions are associated with the Mach wave - airfoil intersection locations and the chordwise distributions aft of the first intersection.

Because the nonuniform airfoil spacing at these conditions primarily affects the pressure difference distribution over the mid and aft chord portions of the airfoil surfaces, the elastic axis location should have a significant effect on the detuning stability enhancement. This is demonstrated in figure 14 which considers the effect of elastic axis location on the stability of the baseline and detuned cascades of these conditions. As seen, as the elastic axis is moved forward of midchord, the improvement in stability due to aerodynamic detuning is increased as compared to a movement of the elastic axis aft of midchord.

It is interesting to consider the fundamental differences between the two cascade configurations at the conditions for which both are neutrally stable, M = 1.32 and k = 1.3 per figure 7. The chordwise variation of the imaginary part of the surface pressures and the pressure differences are presented in figures 15 to 20. As seen, the detuning primarily affects the chordwise distributions of the unsteady pressures on the pressure surfaces of the two reference airfoils (figs. 15 to 18). However, the chordwise distributions of the unsteady pressure difference for the baseline and the detuned cascade configurations are significantly different (figs. 19 and 20) even though their integrated values are equal, i.e., the imaginary part of $C_{\alpha\alpha}$ for each of these configurations is zero. Thus, although the aerodynamic detuning has greatly affected the unsteady aerodynamic loading distributions, the aeroelastic stability has not been affected.

SUMMARY AND CONCLUSIONS

A model for aerodynamic detuning to achieve enhanced supersonic unstalled aeroelastic stability has been developed. This model analyzes the stability of an aerodynamically detuned rotor operating in a supersonic inlet flow field with a subsonic leading edge locus, with the aerodynamic detuning accomplished by means of nonuniform circumferential spacing of adjacent rotor blades. The unsteady aerodynamic forces and moments acting on the blading are defined in terms of influence coefficients in a manner that permits the stability of both a conventional uniformly spaced rotor configuration as well as the detuned nonuniform circumferentially spaced rotor to be determined.

The effect of this aerodynamic detuning on the fundamental unsteady aerodynamics and aeroelastic stability were considered utilizing Verdon's Cascade B as a baseline configuration. This study demonstrated the potential enhanced stability associated with this type of aerodynamic detuning. The aerodynamic detuning significantly affected the chordwise distributions of the unsteady surface pressures. However, aerodynamic detuning did not always affect the unsteady pressure distributions over the complete airfoil chord. For conditions such that the baseline configuration was unstable but the detuned cascade neutrally stable, the effect of aerodynamic detuning on the unsteady pressure differences was shown to be associated with the Mach wave airfoil intersection locations and the chordwise distributions aft of the first intersection. For these conditions, it was then demonstrated that a forward position, as opposed to an aft position, for the elastic axis was associated with increased stability enhancement. It was also shown that for one particular set of conditions, both the uniformly spaced and the aerodynamically detuned cascade configurations were neutrally stable but the associated unsteady surface pressure and pressure difference chordwise distributions were significantly different, i.e., detuning significantly affected the surface pressure distributions but did not enhance the cascade stability.

REFERENCES

1. Whitehead, D.S., "Effect of Mistuning on the Vibration of Turbo-Machine Blades Induced by Wakes," Journal of Mechanical Engineering Science, Vol. 8, No. 1, Mar. 1966, pp. 15-21.

2. Kaza, K.R.V. and Kielb, R.E., "Flutter and Response of a Mistuned Cascade in Incompressible Flow," AIAA Journal, Vol. 20, No. 8, Aug. 1982, pp. 1120-1127.

3. Kielb, R.E., and Kaza, K.R.V., "Aeroelastic Characteristics of a Cascade of Mistuned Blades in Subsonic and Supersonic Flows," Journal of Vibration, Acousitics, Stress, and Reliability in Design, Vol. 105, No. 4, Oct. 1983, pp. 425-433.

4. Bendiksen, O.O., "Flutter of Mistuned Turbomachinery Rotors," ASME Paper 83-GT-153, Mar. 1983.

5. Crawley, E.F. and Hall, K.C., "Optimization and Mechanisms of Mistuning in Cascades," ASME Paper 84-GT-196, June 1984.

6. Verdon, J.M., "The Unsteady Aerodynamics of a Finite Supersonic Cascade with Subsonic Axial Flow," Journal of Applied Mechanics, Vol. 40, No. 3, Sept. 1973, pp. 667-671.

7. Kurosaka, M.K., "On the Unsteady Supersonic Cascade with a Subsonic Leading Edge - An Exact First Order Theory - Parts 1 and 2," Journal of Engineering for Power, Vol. 96, No. 1, Jan. 1974, pp. 13-31.

8. Verdon, J.M. and McCune, J.E., "Unsteady Supersonic Cascade in Subsonic Axial Flow," AIAA Journal, Vol. 13, No. 2, Feb. 1975, pp. 193-201.

9. Brix, C.W., Jr. and Platzer, M.F., "Theoretical Investigation of Supersonic Flow Past Oscillating Cascades with Subsonic Leading - Edge Locus," AIAA Paper 74-14, Jan. 1974.

10. Caruthers, J.E. and Riffel, R.E., "Aerodynamic Analysis of a Supersonic Cascade Vibrating in a Complex Mode," Journal of Sound and Vibration, Vol. 71, No. 2, July 22, 1980, pp. 171-183.

11. Adamczyk, J.J. and Goldstein, M.E., "Unsteady Flow in a Supersonic Cascade with Subsonic Leading-Edge Locus," AIAA Journal, Vol. 16, No. 12, Dec. 1979, pp. 1248-1254.

12. Yates, J.E., "Analysis of Superosnic Unsteady Cascades with the Method of Characteristics," AFFDL-TR-75-159-VOL-1, Aeronautical Research Associates of Princeton, Inc. (ARAP-263), Dec. 1975. (AD-A025909)

13. Ni, R.H. and Sisto, F., "Numerical Computation of Nonstationary Aerodynamics of Flat Plate Cascades in Compressible Flow, Journal of Engineering for Power, Vol. 98, No. 2, Apr. 1976, pp. 165-170.

14. Verdon, J.M., "Further Developments in the Aerodynamic Analysis of Unsteady Supersonic Cascades, Parts 1 and 2," ASME Papers 77-GT-44 and 77-GT-45, Mar. 1977.

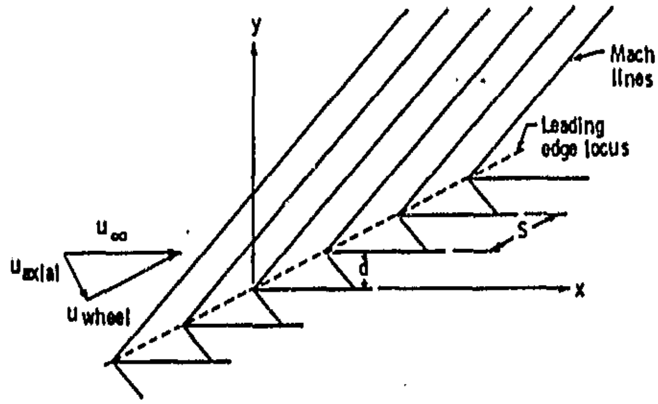

Figure 1. - Flat plate airfoil cascade in a supersonic inlet flow with a subsonic leading edge locus.

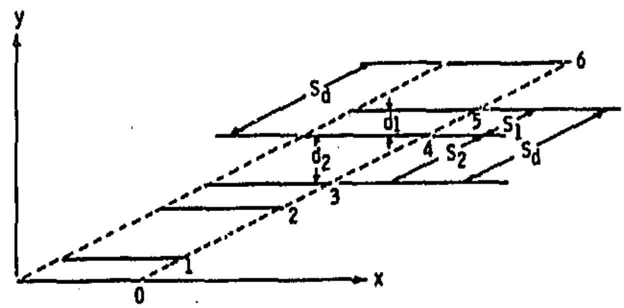

Figure 2. - Finite cascade representation for alternate nonuniform circumferential spacing.

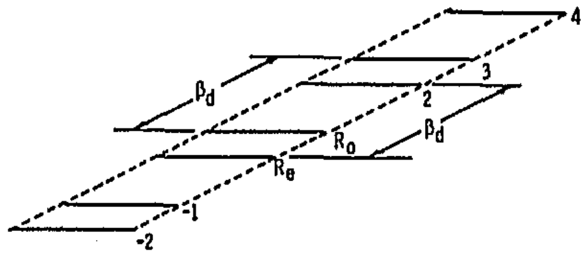

Figure 3. - Reference airfoil passage for nonuniformly spaced cascade.

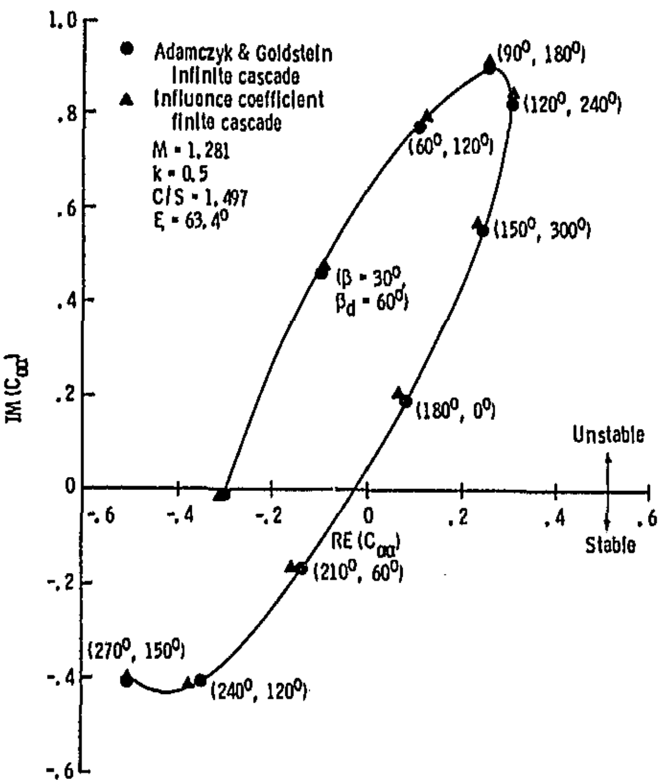

Figure 4. - Comparison of finite cascade influence coefficient model with infinite cascade conventional tuned cascade analysis.

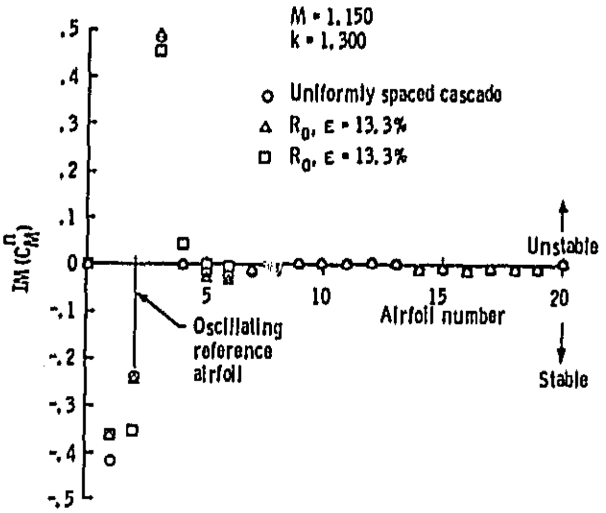

Figure 5. - Influence coefficients for uniform and nonuniform circumferentially spaced cascades.

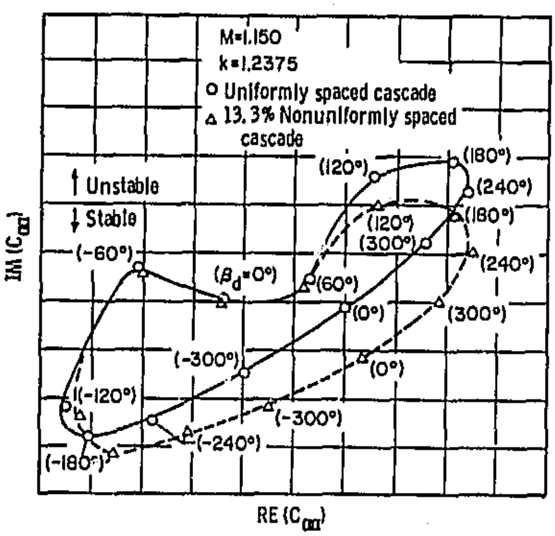

Figure 6. - Effect of aerodynamic detuning on the unsteady aerodynamic moment coefficients.

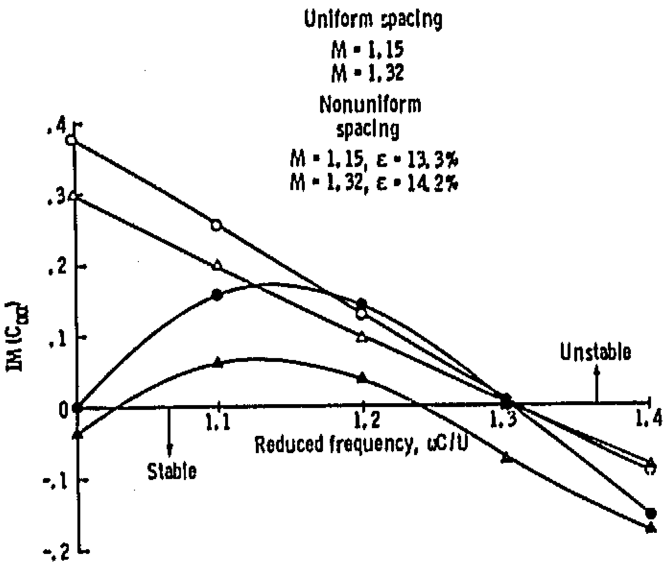

Figure 7. - Effect of inlet Mach number on the stability of the uniform and aerodynamically detuned cascades.

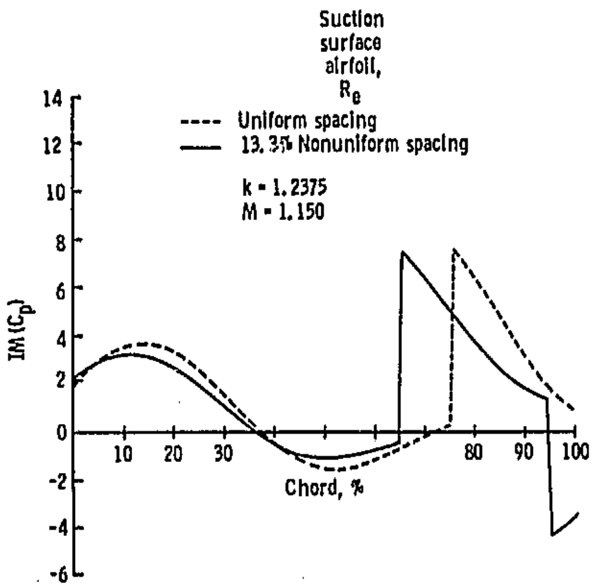

Figure 8. - Airfoil R_e suction surface imaginary unsteady pressure distributions for unstable uniform cascade and neutrally stable detuned cascade.

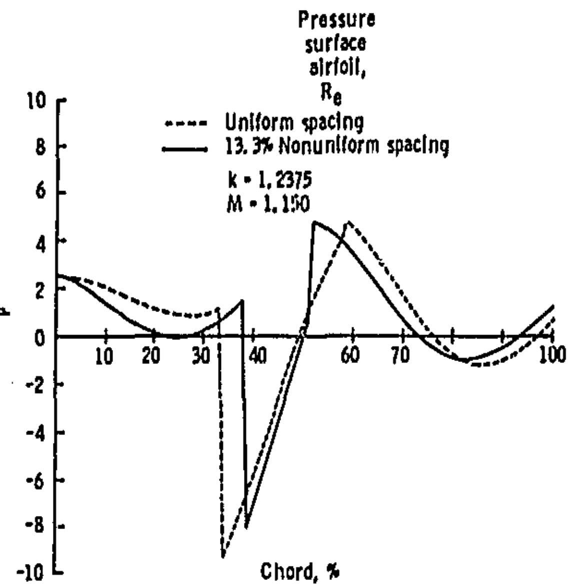

Figure 9. - Airfoil R_e pressure surface imaginary unsteady pressure distributions for unstable uniform cascade and neutrally stable detuned cascade.

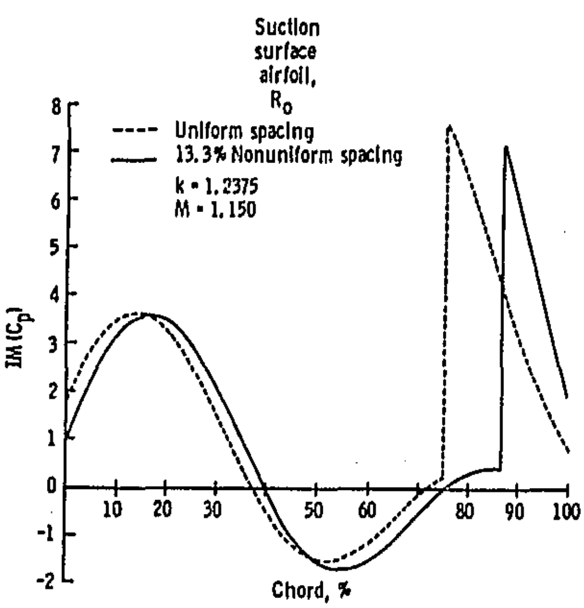

Figure 10. - Airfoil R_o suction surface imaginary unsteady pressure distributions for unstable uniform cascade and neutrally stable detuned cascade.

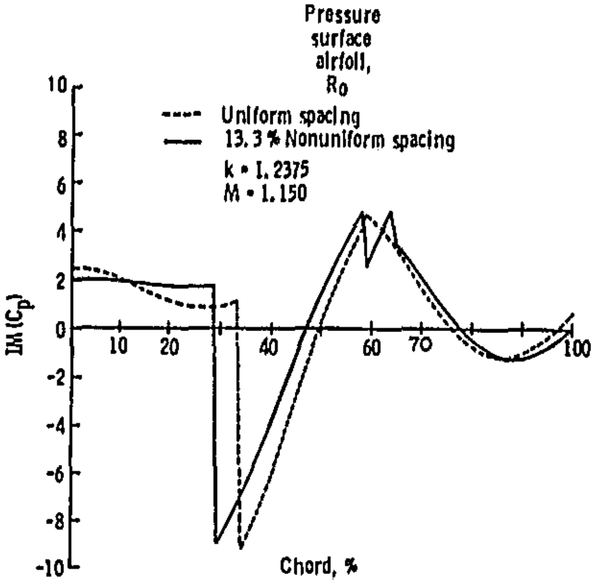

Figure 11. - Airfoil R_0 pressure surface imaginary unsteady pressure distributions for unstable uniform cascade and neutrally stable detuned cascade.

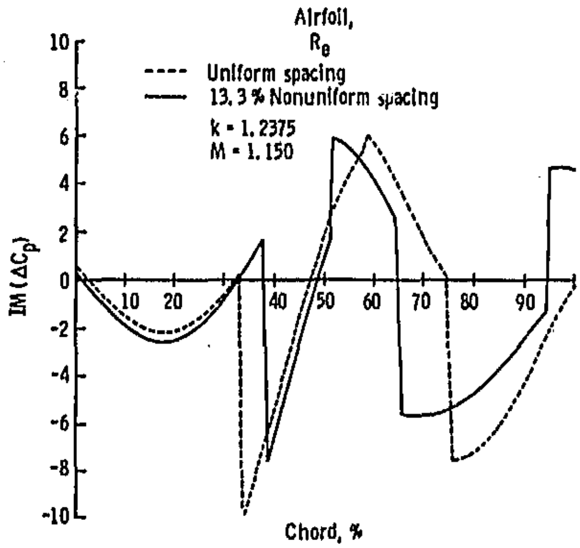

Figure 12. - Airfoil R_e imaginary pressure difference distributions for unstable uniform cascade and neutrally stable detuned cascade.

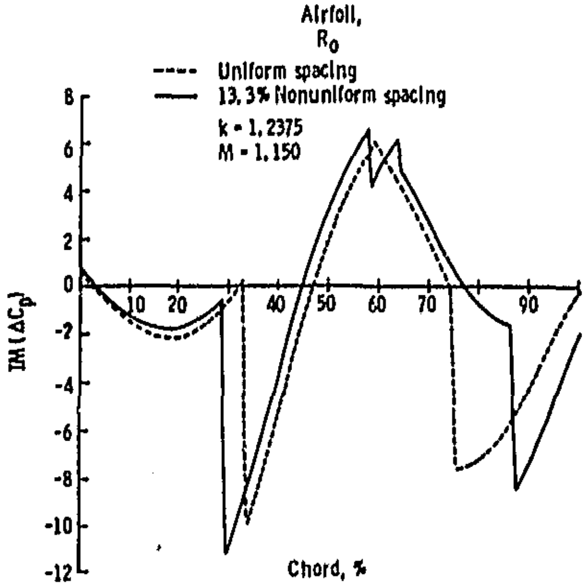

Figure 13. - Airfoil R_0 imaginary pressure difference distributions for unstable uniform cascade and neutrally stable detuned cascade.

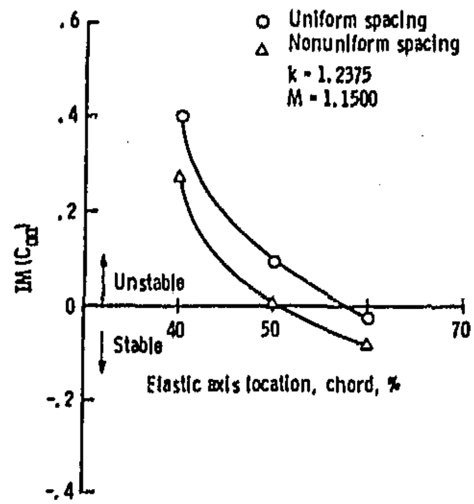

Figure 14. - Effect of elastic axis location on the stability of the uniform and aerodynamically detuned cascades.

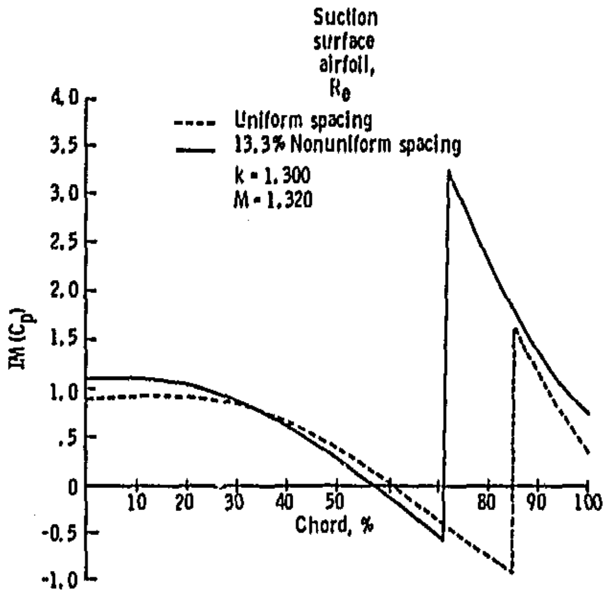

Figure 15. - Airfoil R_e suction surface imaginary pressure distributions for neutrally stable uniform and aerodynamically detuned cascades.

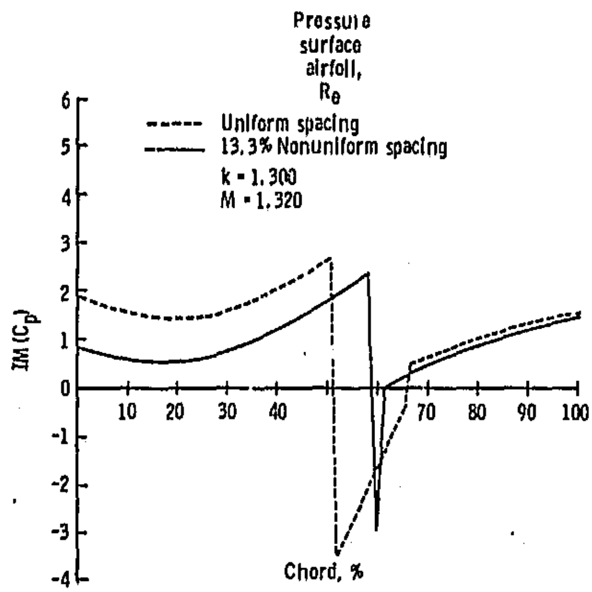

Figure 16. - Airfoil R_e pressure surface imaginary pressure distributions for neutrally stable uniform and aerodynamically detuned cascades.

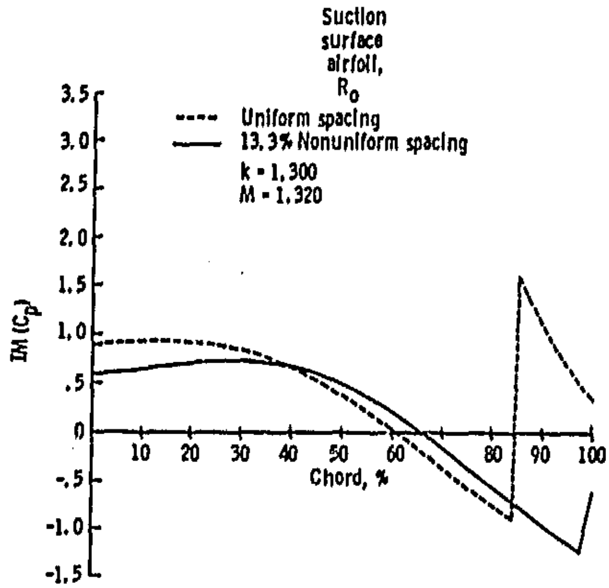

Figure 17. - Airfoil R_0 suction surface imaginary pressure distributions for neutrally stable uniform and aerodynamically detuned cascades.

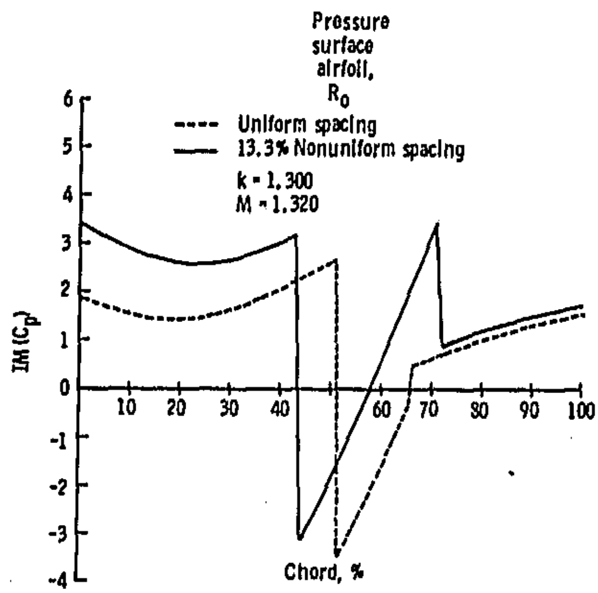

Figure 18. - Airfoil R_0 pressure surface imaginary pressure distributions for neutrally stable uniform and aerodynamically detuned cascades.

ORIGINAL PAGE IS
OF POOR QUALITY

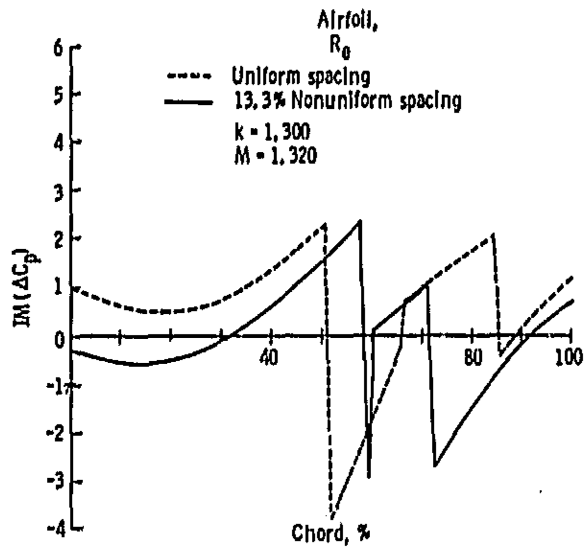

Figure 19. - Airfoil R_e imaginary pressure difference distributions for neutrally stable uniform and aerodynamically detuned cascades.

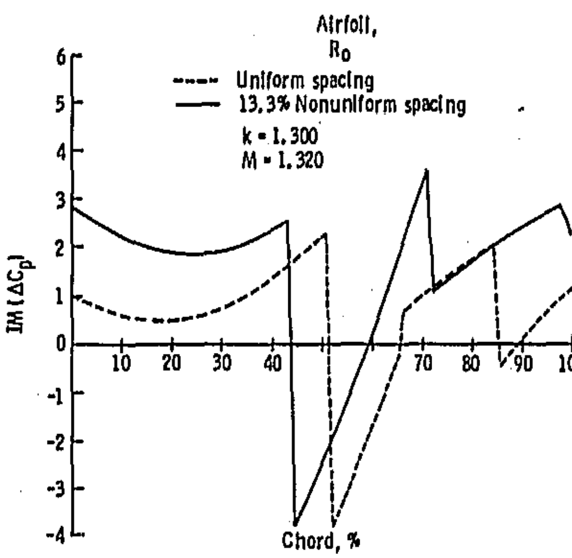

Figure 20. - Airfoil R_0 imaginary pressure difference distributions for neutrally stable uniform and aerodynamically detuned cascades.

1. Report No.	2. Government Accession No.	3. Recipient's Catalog No.
NASA TM-87001		

4. Title and Subtitle	
Aerodynamic Detuning Analysis of an Unstalled Supersonic Turbofan Cascade	5. Report Date
	6. Performing Organization Code 535-05-12
7. Author(s) Daniel Hoyniak and Sanford Fleeter	8. Performing Organization Report No. E-2546
	10. Work Unit No.
9. Performing Organization Name and Address National Aeronautics and Space Administration Lewis Research Center Cleveland, Ohio 44135	11. Contract or Grant No.
	13. Type of Report and Period Covered Technical Memorandum
12. Sponsoring Agency Name and Address National Aeronautics and Space Administration Washington, D.C. 20546	14. Sponsoring Agency Code

15. Supplementary Notes

Daniel Hoyniak, NASA Lewis Research Center; Sanford Fleeter, Purdue University, School of Mechanical Engineering, West Lafayette, Indiana. Prepared for the Thirtieth International Gas Turbine Conference and Exhibit, sponsored by the American Society of Mechanical Engineers, Houston, Texas, March 17-21, 1985.

16. Abstract

A new, and as yet unexplored, approach to passive flutter control is aerodynamic detuning, defined as designed passage-to-passage differences in the unsteady aerodynamic flow field of a rotor blade row. Thus, aerodynamic detuning directly affects the fundamental driving mechanism for flutter, i.e., the unsteady aerodynamic forces and moments acting on individual rotor blades. In this paper, a model to demonstrate the enhanced supersonic unstalled aeroelastic stability associated with aerodynamic detuning is developed. The stability of an aerodynamically detuned cascade operating in a supersonic inlet flow field with a subsonic leading edge locus is analyzed, with the aerodynamic detuning accomplished by means of nonuniform circumferential spacing of adjacent rotor blades. The unsteady aerodynamic forces and moments on the blading are defined in terms of influence coefficients in a manner that permits the stability of both a conventional uniformally spaced rotor configuration as well as the detuned nonuniform circumferentially spaced rotor to be determined. With Verdon's uniformly spaced Cascade B as a baseline, this analysis is then utilized to demonstrate the potential enhanced aeroelastic stability associated with this particular type of aerodynamic detuning.

17. Key Words (Suggested by Author(s))	18. Distribution Statement
Aeroelasticity; Unsteady aerodynamics; Supersonic flutter analysis; Influence coefficients	Unclassified - unlimited STAR Category 02

19. Security Classif. (of this report)	20. Security Classif. (of this page)	21. No. of pages	22. Price*
Unclassified	Unclassified		

*For sale by the National Technical Information Service, Springfield, Virginia 22161